Ecological Indicators 104 (2019) 237–247

Contents lists available at ScienceDirect

Ecological Indicators

journal homepage: www.elsevier.com/locate/ecolind

Instantaneous and long-term CO_2 assimilation of *Platycladus orientalis* estimated from ^{13}C discrimination

Weiwei Lu, Xinxiao Yu*, Guodong Jia

Key Laboratory of State Forestry Administration on Soil and Water Conservation, Beijing Forestry University, Beijing 100083, China

ARTICLE INFO

Keywords:
Sap flow
Gas exchange measurement
Stable carbon isotope discrimination
Tree rings
Stomatal conductance

ABSTRACT

Long-term forest productivity and carbon sequestration capacity are affected by climate change, and have become a global concern. In this study, we provide a simple and nondestructive method to determine tree CO_2 assimilation across multiple time scales. The new method combines sap flow and stable carbon isotope discrimination ($\Delta^{13}C$) measurements to estimate carbon assimilation. We analyzed variability and conducted paired-sample *t*-tests to compare CO_2 assimilation estimated from gas exchange measurements and the new approach to verify its accuracy and applicability. Gas exchange and isotopic measurements both showed that the CO_2 assimilation rate in the morning was higher than in the afternoon, and peak values occurred around 10–11 a.m., which may have been due to nocturnal water storage and higher stomatal conductance in the morning. Diurnal, monthly, and annual CO_2 assimilation of *P. orientalis* variations were related to water supply conditions. Compared with previous research, we experimented using tree-ring stable carbon isotope discrimination ($\Delta^{13}C$) and sap flow measurement to estimate annual CO_2 assimilation and the results were consistent with other traditional methods. *Platycladus orientalis* is effective and responsive to water supply, which explained why it adapts well in semi-arid areas. The new method for estimating CO_2 assimilation was accurate and applicable in semi-arid areas around Beijing.

1. Introduction

Over the last 150 years, the CO_2 content in atmosphere has increased from 280 to 400 μmol mol^{-1}, and has reached 400 μmol mol^{-1} in China and other countries. Rising atmospheric CO_2 is due to excessive emissions generated by land use changes and the burning of fossil fuels, and has resulted in significant changes in global climate (Pachauri et al., 2014; Silva and Horwath, 2013). Forests act as vital CO_2 sinks by storing carbon in woody biomass to balance emissions and sequestration (Nowak et al., 2002; Wang et al., 2014). Long-term forest productivity and carbon sequestration capacity are affected by climate change and have become a global concern (Sun et al., 2010; Battipaglia et al., 2013). However, estimation of CO_2 assimilation on different time and space scale has not been common. Such uncertainties hinder our ability to understand the response of forest to global climate change, as well as to increase CO_2 sequestration through forest management.

Advances in Eddy Covariance (EC) have improved our understanding of H_2O and CO_2 exchange between forest ecosystems and the atmosphere (Baldocchi, 2003; Canadell et al., 2000). However, there are many limitations to the application of EC in measuring carbon sequestration. One is the requirement of a flat landform, which restricts its application in mountainous areas. Current studies on instantaneous carbon sequestration were mostly based on gas exchange and gas chamber monitoring, which adopting branch bag techniques, or combining water-use efficiency obtained with branch bag techniques with whole-tree transpiration (Rayment and Jarvis, 1999; Morén et al., 2001). Gas exchange technology is a commonly used method to identify the photosynthetic characteristics of plant leaves, but can only represent leaf parts at a certain time. Morén et al. (2001) used branch gas chamber and sap-flow techniques to calculate whole-tree water use efficiency and then studied the relationship between photosynthesis and transpiration, finding a strong dependency on the vapor pressure deficit (VPD) (Morén et al., 2001). Catovsky et al. (2002) used sap flow as a measure of whole tree function to examine how the canopy-level transpiration and photosynthetic rates differ between coniferous and broad-leaved species in mixed temperate forests, finding that canopy photosynthesis was more sensitive to VPD and the relationship between photosynthesis and conductance was significant (Catovsky et al., 2002). Application of this method still requires extensive leaf gas exchange measurements, which are time-consuming and difficult. Other methods

* Corresponding author at: Key Laboratory of Soil and Water Conservation and Desertification Combating of the Ministry of Education, Beijing Forestry University, Beijing 100083, China.
E-mail address: yuxinxiao1961@126.com (X. Yu).

https://doi.org/10.1016/j.ecolind.2019.05.007
Received 9 August 2018; Received in revised form 26 April 2019; Accepted 2 May 2019

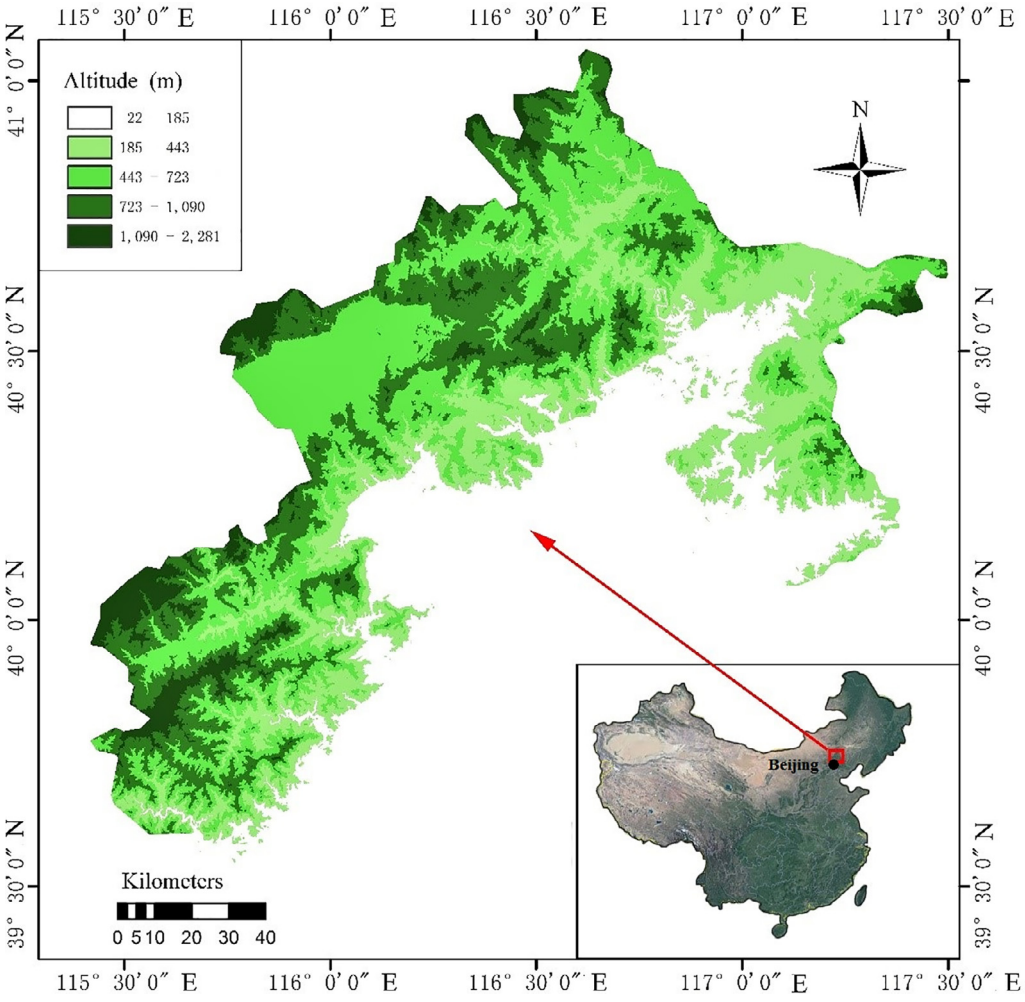

Fig. 1. Geographic location of the study area.

for estimating instantaneous carbon sequestration also have different shortcomings. For example, spectrum technology primarily focuses on measuring instantaneous CO_2 assimilation and the accuracy is concentration dependent (Bowling et al., 2003; Wingate et al., 2010). In addition to the difficulty in estimating the instantaneous carbon sequestration, there are also many uncertainties in estimation of long-term carbon sequestration of forests. Currently, our state of knowledge about the long-term forestry net primary productivity is largely underpinned by traditional methods, such as experimental evidence collected from CO_2 enrichment experiments, palaeorecords, or biomass model. CO_2 uptake varies according to many factors such as tree species, tree age, and resource availability (Oren et al., 2001; Peng, 2003). This necessitates research on how to best estimate long-term forest CO_2 sequestration at the individual and ecosystem scales.

When plants absorb atmospheric CO_2, the carbon isotope effect reduces the ^{13}C content in plants until it is less than that of CO_2 (Dawson et al., 2002; Farquhar et al., 1989). $\delta^{13}C$ is an integrated reflection of photosynthetic activity during leaf formation and is more effective than gas exchange technology as a comprehensive indicator. Carbon isotope analysis can be used to reveal average photosynthesis over spatial and temporal scales (Dawson et al., 2002). Stable carbon isotopic information in different tree organic matter reveals average photosynthetic characteristics during the formation of organic matter, which we referred to as the "scale correspondence rule" (Farquhar et al., 1989; Farquhar and Sharkey, 1982). For example, $\Delta^{13}C$ of leaf soluble organic matter, leaf dry matter, and tree rings reveal average photosynthetic characteristics over days, seasons, and years, respectively. Recently, novel approach combining sap flow measurements and stable carbon isotopes was proposed to estimate canopy CO_2 uptake (Hu et al., 2010; Wang et al., 2014; Zhao and Zhou, 2006). The theory of this method based on the relationship between net carbon sequestration (A_{net}) and canopy stomatal conductance (G_s) established based on stable carbon isotope discrimination ($\Delta^{13}C$). Hu et al. (2010) tested for differences in the carbon isotope ratio of needle sugars and water-use efficiency between sun and shade needles, throughout the growing season, and found observed the highest values of whole-tree CO_2 assimilation rates following snowmelt or summer rain events, and during weather with lower temperatures. Klein et al. (2016) compared long-term CO_2 assimilation in a semi-arid pine forest using eddy covariance (EC) and carbon isotope analysis, and found that there was a good agreement at annual timescales (Klein et al., 2016). However, the method is not widely tested on different tree species or areas either, and there is still a need to measure multi-scale CO_2 assimilation in the context of global climate change, and at the annual scale in particular.

The Yanshan Mountains of northern China lie between the Mongolia Plateau and the North China Plain, and are forested that is dominated by *P. orientalis*. This area plays a significant role in the global carbon cycle due to its typical monsoon climate. *P. orientalis*, an evergreen coniferous tree that is endemic to China, is the main tree species used for afforestation in the semi-arid areas of northern China. Climate change research in China over the last century has focused on the importance of adaptation strategies and productivity of typical evergreen conifers in the semi-arid region of northern China. In this study, we studied *P. orientalis* to derive a simple and nondestructive method for

determining tree CO_2 assimilation across diurnal, seasonal, and annual scales. Compared with previous research, we conducted experiments using tree-ring stable carbon isotope discrimination ($\Delta^{13}C$) and sap flow measurements to estimate annual CO_2 assimilation. The specific goals of this study were to (1) provide a method for estimating stand CO_2 assimilation and compare the results with other methods; and (2) calculate diurnal and annual CO_2 assimilation for individual trees.

2. Materials and methods

2.1. Study area and climate

This study was carried out at the National Forest Ecosystem Research Station (NFERS, 40°03′N, 116°05′E) in Jiufeng National Forest located in the Yanshan Mountains (Fig. 1), a typical rocky mountainous area in northern China (Jijun et al., 2010). The forest in study area was planted in the 1950s with no additional management. It is dominated by *Platycladus orientalis* with a density of 756 trees per ha. *P. orientalis*, is an evergreen coniferous tree that has strong adaptability and resistance to dry and barren conditions. It is mainly distributed in areas with altitudes of 200 m–600 m, along shady and sunny slopes (Wang et al., 2005). This region has an average elevation of 450 m and is characterized by a sub-humid, warm, and temperate continental monsoon climate with average annual temperatures of 11.6 °C and four distinctive seasons: a dry and windy spring, hot and rainy summer, cool and moist autumn, and cold and dry winter. There is dramatic interannual variability in precipitation associated with the monsoon and global climate change, which ranges from 300 mm to 1200 mm (Li et al., 2011). Meteorological data were collected from NFERS and the China Meteorological Administration [http://data.cma.cn/data/index/f0fb4b55508804ca.html].

Two sample plots with a total area of 483.6 were selected along the south-facing (sunny) and north-facing (shady) slopes around 200–300 m in elevation and with gradients around of 14–18°. Photosynthetically active radiation (*PAR*, $\mu mol\ m^{-2}\ s^{-1}$), vapor pressure deficit (*VPD*, kPa), and soil water content (*SWC*, $m^3\ m^{-3}$) are three important factors that influence stomatal conductance (g_s, $mmol\ m^{-2}\ s^{-1}$). *VPD* was calculated as follows (Campbell and Norman, 2012):

$$VPD = 0.611 \times \exp\left[\frac{17.502 \times T_a}{(T_a + 240.97)}\right] \times (1 - RH) \quad (1)$$

PAR, air temperature (T_a, °C) and air relative humidity (*RH*, %) were monitored by an automatic weather station located about 100–120 m away from the study area. The soil type was cinnamon soil with a depth of 40–120 cm (Zhang et al., 2009a). Soil near the surface (0–40 cm) was primarily made up of clay with lower density gravel, and deep soil (> 40 cm) was mainly loam with a higher density of gravel. *SWC* values at soil depths of 30 cm, 60 cm, and 90 cm were measured using soil moisture probes (ML2x, Delta-T Device, UK), and two SWC measurement systems were placed in each plot among the selected trees.

2.2. Sap flow measurement

From 2013 to 2016, TDP (Thermal Dissipation Sapwood Flow Velocity Probe) systems (FLGS-TDP, Dynamax, U.S.A.) were used to measure sap flux density (*Js*, $g\ H_2O\ cm^{-2}\ s^{-1}$). Diameter at breast height (DBH) of trees in the study area varied only slightly, ranging from 17 cm to 19.5 cm in 2013. Therefore, we did not classify the trees based on DBH. Eight trees from each plot were selected for sap flow measurements using TDP systems. Before installing the TDP systems, the sapwood area (A_S) of each tree was measured using an increment borer (CO300, Haglof, Sweden) to take tree cores. Then the two sensor probes were inserted vertically into the sapwood at breast height. In addition, TDP systems were installed on the shady side of each tree trunk to avoid temperature increases as a result of direct sunlight, which would increase measurement error. The upper probe contained an electric heater and the lower probe was a reference without an electric heater. The difference in temperature (ΔT) between the two probes would be the largest (ΔT_m) when there was no sap flow. When transpiration occurred, sap flow transported heat away from the upper probe, changing the ΔT value. Based on Granier's thermal dissipation theory and measured ΔT and ΔT_m, the sap flow rate was directly obtained (Granier, 1987). Then, J_S was calculated as follows:

$$J_S = 119 \times \left[\frac{(\Delta Tm - \Delta T)}{\Delta T}\right]^{1.231} \quad (2)$$

2.3. Stomatal conductance and stand transpiration

Stand transpiration T_S was calculated by the following equation:

$$T_S = J_S \times A_S \quad (3)$$

Continuous observations of sap flow provide a chance to understanding nocturnal sap flux, which has been overlooked in many previous studies (Barbour and Buckley, 2007; Resco de Dios et al., 2016; Zeppel et al., 2014). Nocturnal sap flow is variable across species; although it is low, it provides stem water restoration and storage for transpiration during the day and maintains the water balance, especially for drought resistant trees such as *P. orientalis* (Forster, 2014; Zeppel et al., 2014). Accounting for nocturnal sap flow is therefore important in order to accurately calculate stand transpiration and carbon assimilation. In this study, we used 24 h of sap flux to calculate carbon assimilation for *P. orientalis*.

Many scholars have extended sap flow measurements for canopy transpiration by using the Köstner formulas that were simplified by Whitehead and Jarvis to calculate canopy H_2O stomatal conductance (g_{H2O}) (Addington et al., 2004; Ewers et al., 2007; Granier et al., 1996; Köstner et al., 1992), and then analyzing the sensitivity of stomatal conductance response to environmental factors (mainly VPD and SWC) and T_S regulation mechanisms. However, the application of this formula should satisfy certain assumptions (Ewers et al., 2005, 2007; Köstner et al., 1992; Schäfer et al., 2000): (1) air must be fully flowing and exchanging within the canopy with no clear vertical gradient of vapor pressure deficit; (2) the water vapor conductance of the leaf boundary layer should be much higher than that of the stomatal conductance; (3) the leaf temperature should be equal or close to the air temperature; (4) the contribution of storage water to tree transpiration should be negligible; and (5) xylem water transport resistance from root to canopy should be very small as a result of higher hydraulic conductance. In this study, the above assumptions were satisfied by the needle morphology and crown structure of coniferous trees such as *P. orientalis*, and the application of the formula in China's northern coniferous forest have been confirmed. Based on previous work, we calculated g_{H2O} as the following (Köstner et al., 1992; Wang et al., 2014):

$$g_{H2O} = \frac{G_v \times T_a \times \rho \times T_S}{VPD} \quad (4)$$

where G_v is the modified universal gas constant of water vapor ($0.462\ m^3\ kPa\ K^{-1}\ kg^{-1}$) and ρ is the density of water ($998\ kg\ m^{-3}$).

2.4. Ring-width and carbon isotope measurements for air samples, leaf sap and tree rings

Because of the different physical and chemical properties between isotopes, the difference in isotopic composition between substrates and products is called the isotopic effect (Cernusak et al., 2013; Evans and Von Caemmerer, 2013). The carbon isotope effect occurs during photosynthesis, causing the carbon isotopic composition of plants ($\delta^{13}C_p$) to be far lower than atmospheric carbon isotopic composition ($\delta^{13}C_a$). Isotopic effects during photosynthesis can be expressed by isotopic

discriminant values ($\Delta^{13}C$):

$$\delta = \left(\frac{R_{sa}}{R_{re}} - 1\right) \times 1000‰ \quad (5)$$

$$\Delta^{13}\,C = \frac{\delta^{13}C_a - \delta^{13}C_p}{1 + \delta^{13}C_p/10001} \quad (6)$$

where R refers to the ratio of isotopes ^{13}C to ^{12}C in the sample ('sa') and the reference ['re', compared to the Pee Dee Belemnite (PDB) standard]. A stable carbon isotope analyzer (CCIA-36d-EP, Los Gatos Research Inc., U.S.A.) combined with a profile system has been used for observation of $\delta^{13}C_a$ in 2013–2016. In this instrument, a double reflector was used for off-axis integral cavity output spectroscopy (OA-ICOS), which made long-term field observations possible with a measurement accuracy of 0.1‰. The air injection port was the maximum height of the profile system, 9–13 m above the canopy. The continuous monitoring frequency of $\delta^{13}C_a$ was set to 30 min.

Leaf samples were collected on two representative days every month during 2016 to estimate diurnal CO_2 assimilation. Meteorological data for the last five years in Beijing showed that sunshine duration was approximately half of annual daytime total, which means that there were roughly equal numbers of sunny and shady days. In order to make the annual estimates more accurate, we chose one sunny day and one shady day every month to collect leaf samples. Four sampled trees were selected for each plot, and four clusters of mature leaves were collected from the upper, middle, and lower layers of the canopy respectively on each sampled tree every two hours during the day, and then they were immediately wrapped in tinfoil and stored in liquid nitrogen. Sampling time was set according to the time of sunrise and sunset in each month, and samples collected at the same time in the sampling two days from the same tree were mixed together, and eight leaf samples were collected every two hours. The extraction method of soluble organic matter from the leaves followed that of a previous study (Boegelein et al., 2012). The extracted samples were then wrapped in tin capsules for leaf soluble organic matter stable carbon analysis ($\delta^{13}C_{ls}$) using a high temperature reactor (HT-O, HEKAtech GMBH, Wegberg, Germany) coupled with a DELTAplus XP Mass Spectrometer (ThermoFinnigan, Thermo Fisher Scientific Inc., Waltham, MA, U.S.A.).

Two cores were taken from each sampled tree at breast height (1.3 m) along different sections of the stem using a 5-mm increment borer in May 2017. To prevent contamination from other carbon sources, the collected samples were stored in glass tubes. The cores were bound to special woody grooves to prevent bending and dried in the oven at 176 °F for 12 h. Then the core samples were sanded with grain paper from 400 to 1200 mesh in size to make the tree rings more clearly visible for cross-dating. Tree ring widths were measured at a resolution of 0.01 mm from each of the cores using LINTAB 6 measurement equipment (Frank Rinn Inc., Heidelberg, Germany) and the data were analyzed using a Time Series Analysis and Presentation (TSAP) software package (Frank Rinn Inc., Heidelberg, Germany). Cross-dating of the tree ring data was verified using COFECHA, which assesses the quality of cross-dating and the measurement accuracy of a tree ring series using a segmented time-series correlation technique (Holmes, 1983; Nock et al., 2011). After finishing tree ring width measurements the cores were divided into individual rings from 2013 to 2016, using a scalpel to cut along ring lines under a stereomicroscope (40× magnification) and rings within the same year were pooled (Leavitt, 2008; Liu et al., 2012; Maseyk et al., 2011; Szymczak et al., 2012; Woodley et al., 2012; Wu et al., 2015). Earlywood and latewood were not separated for the isotopic analyses, as recent studies have shown that there is no difference between the two wood types at the isotopic level (Borella et al., 1998; Di Matteo et al., 2010). Each pooled sample was ground into a powder using a ball mill (MM-400, Retsch GmbH, Hann, Germany). We extracted the wood cellulose of annual tree rings following Loader (Loader et al., 1997). Then we measured carbon isotopic composition of cellulose samples ($\delta^{13}C_c$) using a high temperature reactor (HT-O, HEKAtech GMBH Inc., Wegberg, Germany) coupled with a DELTAplus XP Mass Spectrometer (ThermoFinnigan, Thermo Fisher Scientific Inc., Waltham, MA, U.S.A.).

2.5. CO_2 assimilation rate estimation

The relative rates of carbon fixation and stomatal conductance are the primary factors that determine $\Delta^{13}C$.

$$\Delta^{13}\,C = a + (b - a)\frac{C_i}{C_a} \quad (7)$$

where a is the discrimination against $^{13}CO_2$ during CO_2 diffusion through the stomata (a = 44‰), b is the discrimination associated with carboxylation (b = 27‰), and C_i and C_a are the intercellular and ambient CO_2 concentrations, respectively. The C_i/C_a ratio represents the relationship between CO_2 assimilation (A) and stomatal conductance of CO_2 (g_{CO2}) which is known as "Fick's law":

$$A = g_{CO_2}(C_a - C_i) \quad (8)$$

The stomatal conductance of water vapor (g_{H2O}) is 1.6 times that the conductance of CO_2, and the change in $\Delta^{13}C$ can be related to the A/g_{H2O} ratio as follows:

$$\Delta^{13}\,C = a + (b - a)\left(1 - 1.6\frac{A}{C_a g_{H_2O}}\right) \quad (9)$$

The relationship between A and g_{H2O} is defined as the intrinsic water-use efficiency (iWUE) (McCarroll and Loader, 2004; Osmond et al., 2012; Robertson et al., 2008):

$$iWUE = \frac{A}{g_{H_2O}} \quad (10)$$

Combining Eqs. (8), (9), and (10), $\Delta^{13}C$ was converted to iWUE, defined as the following:

$$A = g_{H_2O} \times C_a \frac{b - \Delta^{13}C}{1.6(b - a)} \quad (11)$$

where A is the total accumulation of CO_2. Combined with Eq. (4), the CO_2 assimilation rate at the stand scale was established. The understory vegetation was made up of primarily small shrubs and grass, including *Vitex negundo*, *Grewia biloba*, *Oplismentls undulatifolius*, *Rubia cordifolia,* and *Chenopodium album*. The average coverage for understory vegetation was approximately 3–8%, so its influence on *P. orientalis* CO_2 uptake was negligible and we did not account for it in the estimation. Eq. (11) was based on the scale correspondence rule, the $\Delta^{13}C$ of leaf soluble organic matter and tree rings, so the calculated values for A represented daily and annual CO_2 assimilation, respectively. Therefore, we used different sampled materials to estimate A over different time scales.

2.6. Other CO_2 assimilation measurements

To verify the accuracy of Eq. (11), we also calculated CO_2 assimilation using traditional methods, including gas exchange measurements and a biomass model. A portable infrared gas analyzer (Li-Cor 6400, Li-Cor Inc., Lincoln, NE, USA) was used to measure instantaneous water and carbon exchange of plant leaves (individuals or groups), a common method that is simple, convenient, and fast. We measured the physiological factors of plants such as net photosynthetic rate (P), stomatal conductance (g_s), and intercellular CO_2 concentration (Ci) using Li-Cor 6400 before the leaves were collected for stable carbon isotope determination on two representative days of every month in 2016. The measured P values every two hours were considered to be the average net photosynthetic rate for that two hours. Then the measured net photosynthetic rate at per unit leaf area was converted to net CO_2

assimilation rate (A) at canopy level as follows:

$$A = \mathrm{P}\times \mathrm{F}\times \mathrm{LAI} \quad (12)$$

where F is crown area; LAI is leaf area index, which was measured by LAI-2200 (Li-Cor Inc., Lincoln, Nebraska, USA). Therefore, we were able to calculate the net CO_2 assimilation (A) for every two hours and then summed the values to obtain diurnal net CO_2 assimilation (A_d).

The traditional long-term (yearly) CO_2 assimilation calculation method uses a biomass model as follows:

$$W_n = a(D_n^2 H_n)^b - a(D_{n-1}^2 H_{n-1})^b \quad (13)$$

$$An = W_n \times C_c/R_c \quad (14)$$

where W_n is biomass for the n^{th} year (kg); a, b are the empirical parameters 12.419 and 0.795 (Zhang, 2012); D_n is the DBH of tree for the n^{th} year (dm); H_n is tree height for the n^{th} year (m); A_n is the net CO_2 assimilation for the nth year (kg); and C_c is the carbon content of *P. orientalis* (0.5) (Johnson and Sharpe, 1983; Zhang et al., 2009b; Zhao and Zhou, 2006). R_c is the relative mass ratio of carbon atoms to carbon dioxide molecules (3/11).

Here we selected two methods to verify annual CO_2 assimilation inferred from tree ring $\delta^{13}C_c$. One method was traditional long-term (annual) CO_2 assimilation calculations (Eqs. (13) and (14)). The other was self-authentication in 2016. We took the CO_2 assimilation values inferred from $\delta^{13}C_{ls}$ on typical days from each month as the average daily CO_2 assimilation rate for that month in 2016, and then converted them to monthly values by multiplying it by the number of days in that month. Finally, monthly values were summarized to obtain annual CO_2 assimilation for 2016.

2.7. Statistical analysis

All statistical analyses were conducted using SPSS version 11.0 statistical software package (SPSS, Chicago, IL, USA). Variation analysis and paired-sample *t*-test with a null hypothesis of no significance were used to compare the differences between the two time series of CO_2 assimilation values estimated from $\delta^{13}C$ and gas exchange measurements, and quantify the error at a significance level of 0.05.

3. Results

3.1. Microclimate and stand transpiration

Monthly soil water content (SWC) at three soil depths, precipitation (P), air temperature (T), vapor pressure deficit (*VPD*) and photosynthetically active radiation (PAR) in the study area from 2013 to 2016 are shown in Fig. 2. SWC curves clearly fluctuated both within and between years. Monthly SWC values at 30 cm depth were significantly correlated with monthly P ($r = 0.765^{**}$, $p < 0.01$). However, due to the low SWC, deeper soil only received water supply if precipitation was sustained for days or happened frequently. Therefore, there was hysteresis in SWC with increasing soil depth and the Pearson correlation coefficients (r) between deeper SWC and P values were smaller. The average annual precipitation in the study area from 2013 to 2016 was 521.75 mm. Monthly air temperatures had similar patterns between years during the study period with an average value of 13.5 °C and no distinct trend. The inter-annual variability of *VPD* and PAR was relatively small, and monthly values ranged from 0.17 to 1.85 and from 202 to 1023, respectively.

The stand transpiration (T_s) values from 2013 to 2016 for 16 sampled trees are shown in Fig. 3. We monitored the stand transpiration of 16 trees, eight of which were growing along a sunny slope and eight growing along a shady slope. The average transpiration rates are shown in Fig. 3(a) and the individual monthly stand transpiration are shown in Fig. 3(b). There was significant seasonal variability in the stand transpiration of *P. orientalis* that intensified during summer and evened out during winter, which was consistent with PAR, *VPD*, and SWC. The monthly T_s patterns for each year were similar and no significant inter-annual variability was observed during the study period.

3.2. Hourly transpiration and CO_2 assimilation along different aspects

The hourly mean transpiration (T_h) values of sampled trees (n = 16) for every month during 2016 are shown in Fig. 4. There was much higher transpiration in trees growing on sunny slopes than those growing on shady slopes, with the largest diurnal difference of 10,746 g observed in July. Monthly variations were similar between the two slopes, which first increased and then decreased; however, monthly transpiration variability on sunny slopes was much greater than on shady slopes. It can be seen in Fig. 4 that regardless of whether the slope was sunny or shady, transpiration was mainly concentrated between 9 a.m. and 3 p.m. In addition, there was approximately 28.64% more transpiration in the morning than in the afternoon. An interesting observation was that there was a small amount of nocturnal sap flow, which accounted for 7% of all-day transpiration.

The monthly $\delta^{13}C_{ls}$ values for trees growing on sunny and shady slopes in 2016 are shown in Fig. 5. On both sunny and shady slopes, $\delta^{13}C_{ls}$ exhibited a parabolic trend that was higher during the growing season with a maximum value in May, and lower values outside the growing season with a minimum in January. The hourly mean CO_2 assimilation (A_h) of experimental trees for every month of 2016 are shown in Fig. 6. Similar to transpiration, monthly CO_2 assimilation also increased during the first part of the year and then decreased, showing strong seasonality. However, there was a spike in CO_2 assimilation between June and July on both sunny and shady slopes, increasing from 17.25 g and 12.87 g to 28.49 g and 18.74 g, respectively, and the increase along sunny slopes was larger than along shady slopes. There was lower variability of A_h along shady slopes than along sunny slopes. The CO_2 assimilation of trees growing on sunny slopes was much larger than shady slopes, with the largest diurnal difference of 8.43 g in July. CO_2 assimilation was mainly concentrated between 9 a.m. and 3 p.m. In contrast with T_h, there was no significantly difference in CO_2 assimilation on sunny slopes between the morning and afternoon, but slightly more occurred in the morning along shady slopes.

3.3. CO_2 assimilation estimates from gas exchange measurements

The hourly mean CO_2 assimilation of sampled trees estimated using a portable infrared gas analyzer (Li-Cor 6400) for every month of 2016 and the percentages of A_{6400} and A'_{6400} are shown in Fig. 7. Monthly variability was similar between the two slopes, which first increased and then decreased, showing strong seasonality. However, monthly variability of CO_2 assimilation variability on sunny slopes was much greater than on shady slopes. We can see that hourly mean CO_2 assimilation was higher from May to October when the maximum CO_2 assimilation rate was greater than 1 g h^{-1}. The percentages of A_{6400} and A'_{6400} are shown in the pie chart (Fig. 7). The CO_2 assimilation rates of trees growing on sunny slopes were 46.49% higher than on shady slopes.

3.4. Comparison with other measurements

Comparison of hourly mean CO_2 assimilation of sampled trees estimated from ^{13}C discrimination (A_h and A'_h) and portable infrared gas analyzer (A_{6400} and A'_{6400}) was shown in Fig. 8. As can be seen from the Fig. 8, the ratio of carbon sequestration per hour measured from the two methods are close to 1. The difference of hourly mean CO_2 assimilation measured from the two methods of shady slope is greater than that of sunny slope. To validate hourly mean CO_2 assimilation derived from sap flow measurements and stable carbon isotope discrimination, we conducted paired-samples *t*-test between estimated and measured CO_2 assimilation (Table 1). The test results showed that there

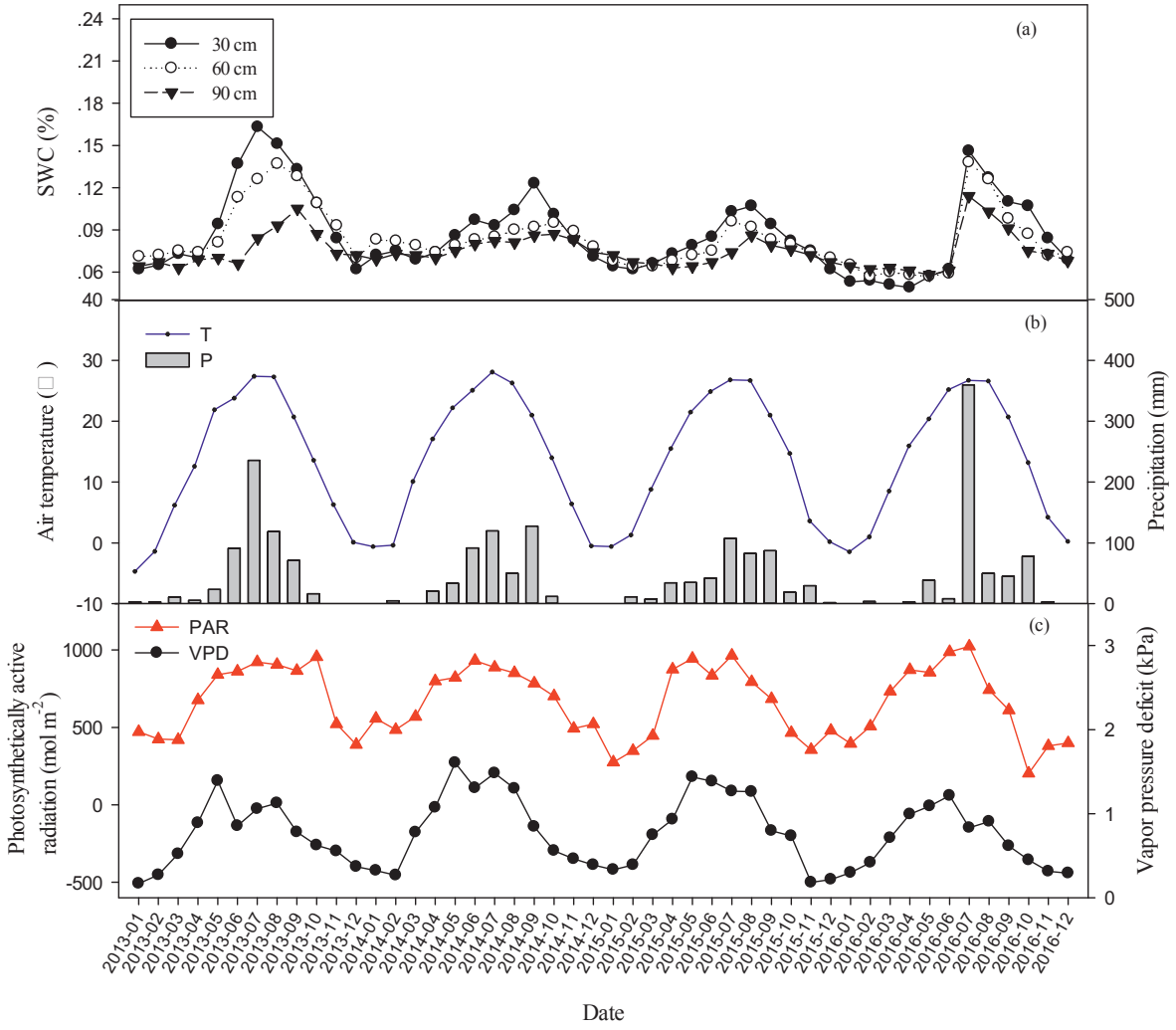

Fig. 2. (a) Monthly soil water content (SWC) at 30 cm, 60 cm and 90 cm soil depths in the study area (2013–2016); (b) Monthly precipitation (P) and average air temperature (T_a) in the study area (2013–2016); (c) Averaged monthly vapor pressure deficit (*VPD*) and photosynthetically active radiation (PAR) in the study area (2013–2016).

was no significant (p_{sunny} = 0.919, p_{shady} = 0.576) difference between the two methods on sunny or shady slopes, and therefore the method combining stable carbon isotope discrimination and sap flow measurements to estimate tree stand hourly mean CO_2 assimilation was reliable.

Annual CO_2 assimilation rates on sunny and shady slopes estimated by the three methods are shown in Table 2. BM from 2013 to 2016 was calculated via Eqs. (12) and (13) based on tree ring widths. In addition, we compared the CO_2 assimilation estimated from SFTD and SFLD in 2016. Details on the calculations can be found in the materials and methods section. Comparing BM and SFTD revealed that CO_2 assimilation estimated from BM was lower than SFTD from 2013 to 2016 with a maximum difference of 3.13%, except on shady slopes in 2014 and 2015. This gap was larger in years when trees grew more rapidly, as in 2012 and 2016. The differences between SFTD and SFLD were slightly larger on shady slopes.

4. Discussion

4.1. Temporal patterns of CO_2 assimilation and transpiration

The results of both gas exchange and isotopic measurements showed that the CO_2 assimilation rate in the morning was higher than in the afternoon and peak values occurred around 10–11 a.m. This result was consistent with the findings of Ainsworth and Long (2005), who found that the carbon uptake rate of soybean was much higher in the morning than in the afternoon with a peak at approximately 11 a.m. In addition, we observed nocturnal sap flow, which meant that *P. orientalis* absorbed water from the soil at night and stores it. Nocturnal water storage is an adaptive strategy during water stress to ensure effective physiological activities in the morning, so peak CO_2 assimilation rates mostly occur in the morning (Matheny et al., 2015). It is precisely because of the arid and barren environment that naturalized *P. orientalis* seize every opportunity to store water, absorb more CO_2, and therefore continue to exist. Niinemets et al. (2011) found that evergreens are better adapted to water shortages, which could further explain *P. orientalis* adaptability in the semi-arid area (Niinemets et al., 2011). The sharp peak may also have been due to higher Gs and Ca, as well as lower Δ, in the morning. Air relative humidity was highest in the morning and then gradually decreased on sunny days. This diurnal pattern was similar to that of canopy conductance on well-watered nine-year-old *Sultana grapevines* (Lu et al., 2003), native forest composed of *Lomatia hirsuta*, *Schinus patagonicus*, *Nothofagus Antarctica* and *Diostea juncea* (Fernández et al., 2009), and pristine *Nothofagus* forest (Köstner et al., 1992).

4.2. Applicability and accuracy

The estimated average annual CO_2 assimilation results for

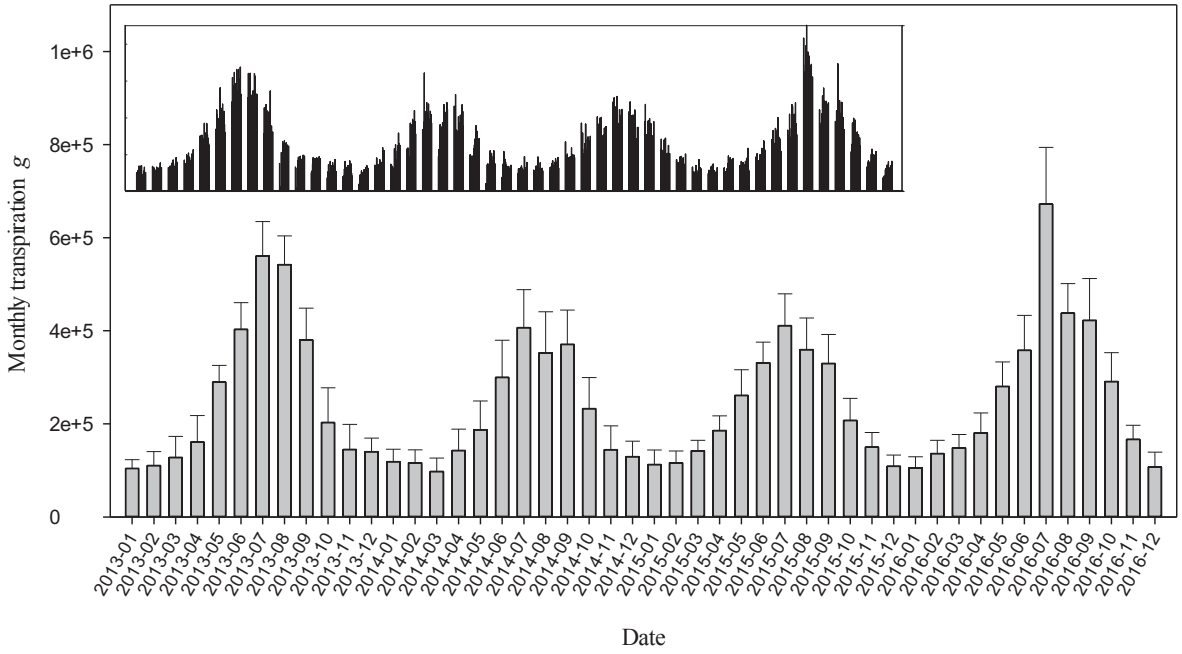

Fig. 3. (a) Average monthly stand transpiration (T_s) of sampled trees (n = 16) from 2013 to 2016, and error bars indicate standard deviation (n = 16); (b) Monthly stand transpiration for each sampled tree from 2013 to 2016.

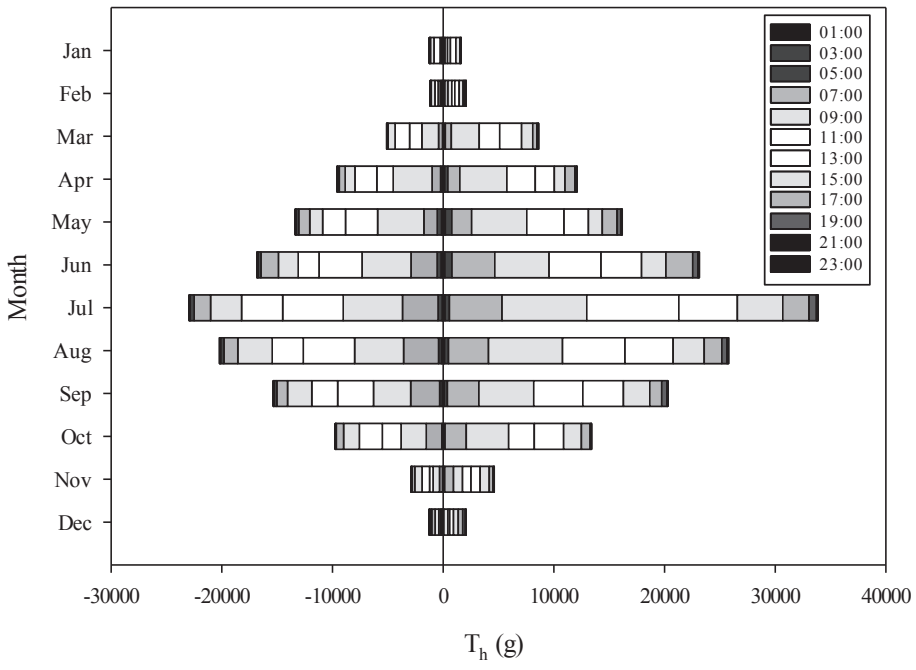

Fig. 4. The hourly mean transpiration (T_h) values for sampled trees (n = 16) measured by TDP systems for each month in 2016. The absolute value of a negative number represents the mean transpiration of eight trees growing along shady slopes and positive values represent the transpiration of eight trees grown along sunny slopes.

individual trees on sunny and shady slopes from 2013 to 2016 based on sap flow measurements and ^{13}C discrimination were 2666.41 g/a^{-1} and 1940.44 g/a^{-1}, respectively (Table 2). These differences may have been the result of many factors, such as calculation methods, tree age, and site conditions. In addition, they could mean that productivity of trees growing in semi-arid and rocky mountainous areas in Beijing have decreased due to climate change, with rising annual air temperatures and fluctuating precipitation (Weiwei et al., 2018). In addition, our estimated results were consistent with Zhang (2012), who calculated NPP based on a biomass model for *P. orientalis* in Beijing (Zhang, 2012). This meant that the new CO_2 assimilation approach could be applicable in Beijing's mountainous areas.

We collected leaf samples on two representative days of each month in 2016 to estimate diurnal CO_2 assimilation. Numerous other studies only collected samples on typical sunny days (Hu et al., 2010; Wang et al., 2014), which could cause errors in calculating monthly or annual CO_2 assimilation due to significant differences between sunny and cloudy days or other weather conditions. Therefore, we chose one sunny day and one shady day every month to collect leaf samples according to the meteorological data over the last five years in Beijing. Wang et al. (2014) estimated canopy CO_2 assimilation for a mature *Acacia mangium* plantation to be 2.13 ± 0.40 g C m^{-2} d^{-1}, which approached the lower range of values for subtropical mixed forests (Gebremichael and Barros, 2006; Gu et al., 2006). Their lower estimates of CO_2 assimilation may have been due to lower mean canopy stomatal conductance, higher Ci/Ca, taller tree height, and lower LAI, compared

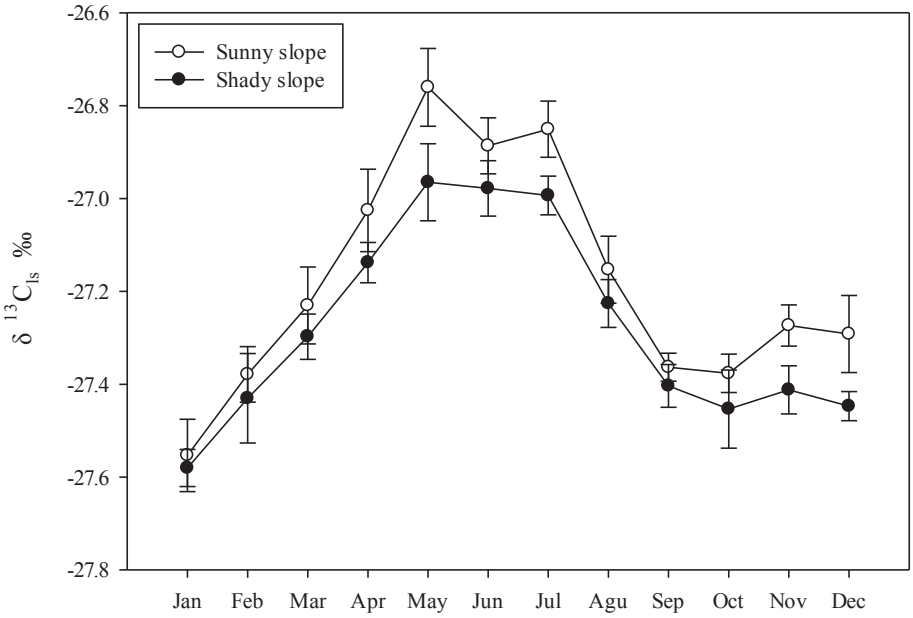

Fig. 5. Monthly $\delta^{13}C_{ls}$ of trees growing on sunny and shady slopes in 2016. Each point represents the mean $\delta^{13}C_{ls}$ of two representative days every month. Error bars indicate the standard error of the mean values.

to other subtropical mixed forests (Gebremichael and Barros, 2006; Ma, 2008). The canopy stomatal conductance of individual trees decreased with tree height, while the lower LAI may have led to higher conductance and more control by stomatal conductance because there was less shading (Granier et al., 2000; Schäfer et al., 2000). We conducted paired-samples *T* tests to verify the reliability and accuracy of hourly mean CO_2 assimilation estimated from sap flow measurements and stable carbon isotope discrimination. The test results illustrated that the method combining stable carbon isotope discrimination and sap flow measurements to estimate hourly mean CO_2 assimilation was reliable and accurate.

4.3. Applications in forestry

Forests growing at northern mid-latitude sites are large CO_2 sinks (Ciais et al., 1995). Some scholars have found that in China, planted forests (afforestation and reforestation) have sequestered 0.45 petagrams of carbon (Fang et al., 2001). *P. orientalis* is the main tree species used for afforestation in the semi-arid areas of northern China. In previous studies (Weiwei et al., 2018), long-term water use efficiency and the basal area increment (BAI) of *P. orientalis* have increased under elevated CO_2 concentrations and rising temperatures. This is mainly because of the special leaf structure, i.e., photosynthetic limitation by mesophyll diffusion varies strongly with leaf structure (Niinemets et al., 2009). Furthermore, *P. orientalis*, supports numerous leaf age classes, leading to high leaf-area indices as 8–13 $m^2\,m^{-2}$ on a projected leaf

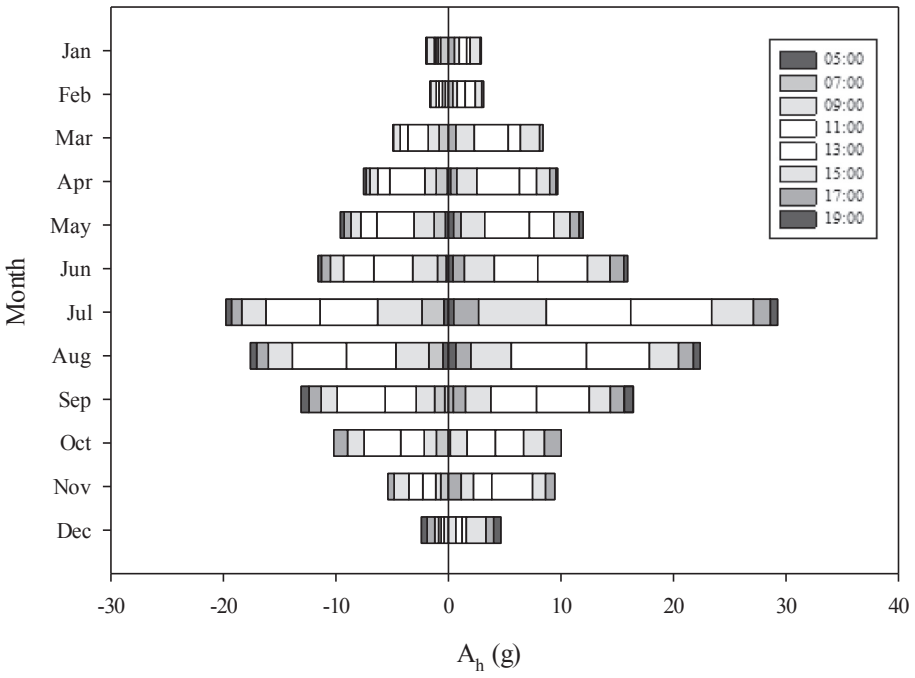

Fig. 6. Hourly mean CO_2 assimilation (A_h) of sampled trees for every month in 2016, estimated from T_h and leaf $\delta^{13}C_{ls}$. The absolute value of a negative number represents the mean CO_2 assimilation of eight trees growing along shady slopes and positive values represent the CO_2 assimilation of eight trees grown along sunny slopes.

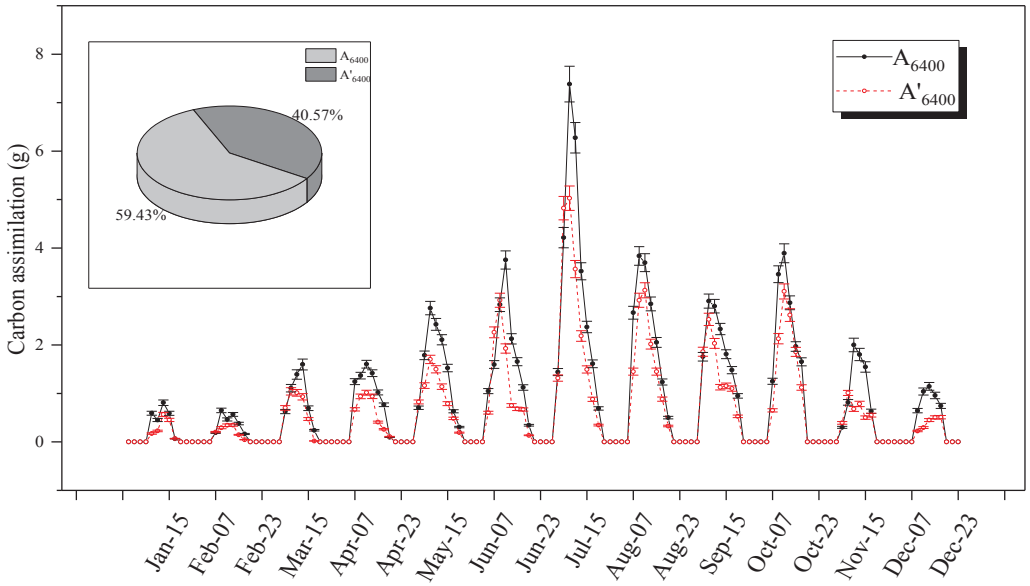

Fig. 7. Hourly mean CO_2 assimilation of sampled trees estimated using a portable infrared gas analyzer (Li-Cor 6400) every month in 2016. The red dotted line is the mean CO_2 assimilation of trees growing along shady slopes (A'_{6400}) and the solid line is the mean CO_2 assimilation of trees growing along sunny slopes (A_{6400}). The percentages of A_{6400} and A'_{6400} are shown in the pie chart.

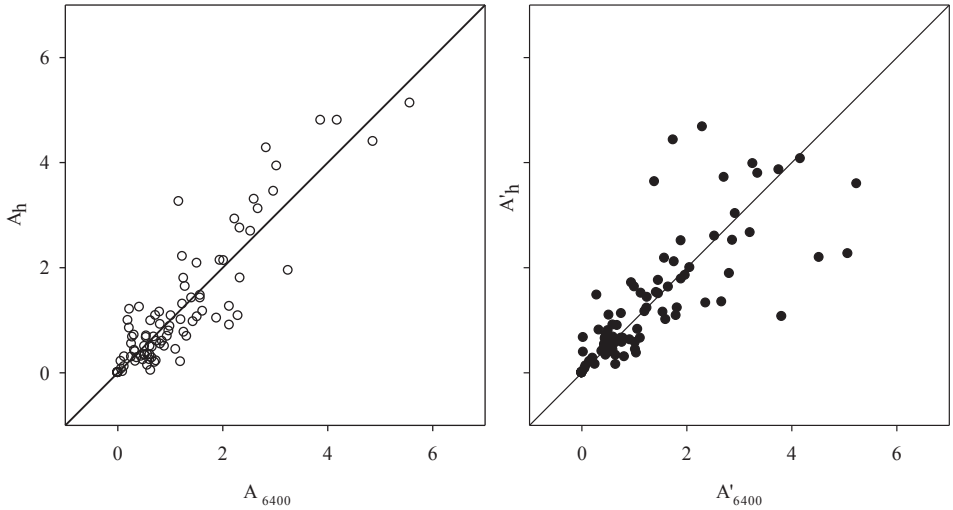

Fig. 8. Comparison of hourly mean CO_2 assimilation of sampled trees estimated from ^{13}C discrimination (A_h and A'_h) and portable infrared gas analyzer (A_{6400} and A'_{6400}). A_h and A_{6400} are CO_2 assimilation of trees growing along sunny slopes; A'_h and A'_{6400} are CO_2 assimilation of trees growing along shady slopes.

Table 1
Paired-samples *T* tests between the hourly mean CO_2 assimilation derived from $\delta^{13}C_{ls}$ and measured by Li-6400.

		Paired Differences					t	df	Sig. (2-tailed)
		Mean	SD	SE Mean	95% confidence interval of the difference				
					Lower	Upper			
Pair 1	Sunny	0.00556	0.53450	0.05455	−0.10274	0.11386	0.102	95	0.919
Pair 2	Shady	0.05025	0.87783	0.08959	−0.12762	0.22811	0.561	95	0.576

Table 2
Annual CO_2 assimilation on sunny and shady slopes calculated using the biomass model (BM), sap flow and tree-ring ^{13}C discrimination (SFTD), and sap flow and foliar soluble organic matter ^{13}C discrimination (SFLD).

Aspects	Years and Methods								
	2013		2014		2015		2016		
	BM	SFTD	BM	SFTD	BM	SFTD	BM	SFTD	SFLD
Sunny slope	2828.15	2963.71	2016.39	2039.58	1705.43	1885.62	3643.54	3776.72	3768.35
Shady slope	2193.98	2204.18	1527.54	1494.96	1435.85	1411.04	2393.66	2651.58	2709.71

area basis (Niinemets, 2010). With a more robust leaf structure, typical reductions in stomatal conductance observed in response to elevated CO_2 are likely to reduce photosynthesis, and generate a stronger iWUE response. However, uncertainties hinder our ability to estimate long-term forest CO_2 sequestration for global carbon budgets, as well as to increase CO_2 uptake rate through forest management. In this study, we combined sap flow and $\Delta^{13}C$ measurements to estimate instantaneous and long-term CO_2 assimilation, and found that *P. orientalis* is effective and responsive to water supply, which explains why it adapts well to semi-arid areas. In the context of climate change, the eco-physiological functions of the *P. orientalis* forest ecosystem are maintained and have a high potential for carbon sequestration. In addition, the method proposed in this study can help researchers better understand the CO_2 assimilation history of different trees, compare the CO_2 sequestration potential of different species and forest types, and make appropriate adjustments in forest management to adapt to future climate change. Our study findings will be useful in constraining global carbon budgets and allow researchers to measure forestry productivity over the years and under various climate regimes, which could be used to improve forest management and conservation practices.

5. Conclusions

Our study verified the applicability and accuracy of an approach that combined sap flow measurements and ^{13}C discrimination to estimate stand CO_2 assimilation rates across different time scales. CO_2 assimilation was higher on sunny slopes than on shady slopes. The results from gas exchange and isotopic measurements showed that the CO_2 assimilation rate in the morning was higher than in the afternoon with peak values occurring around 10–11 a.m., which may be due to nocturnal water storage and higher stomatal conductance in the morning. Variability in diurnal, monthly, and annual CO_2 assimilation of *P. orientalis* was related to water supply conditions. *P. orientalis* is effective and responsive to water supply, which explains why this species adapts well in semi-arid areas. In addition, this method will allow researchers to identify the appropriate species in each region around the world to maximize CO_2 uptake, while remaining cognizant of the coupled water-carbon cycle and processes in terrestrial ecosystems.

Acknowledgements

This research was supported by the National Natural Science Foundation of China (Nos. 41430747 and 41877152) and the Beijing Municipal Education Commission (No. CEFF-PXM2018_014207_000024). All experiments were conducted in compliance with the current laws of the country in which they were performed.

References

Addington, R.N., Mitchell, R.J., Oren, R., Donovan, L.A., 2004. Stomatal sensitivity to vapor pressure deficit and its relationship to hydraulic conductance in Pinus palustris. Tree Physiol. 24, 561–569.

Ainsworth, E.A., Long, S.P., 2005. What have we learned from 15 years of free-air CO_2 enrichment (FACE)? A meta-analytic review of the responses of photosynthesis, canopy properties and plant production to rising CO_2. New Phytol. 165, 351–372.

Baldocchi, D.D., 2003. Assessing the eddy covariance technique for evaluating carbon dioxide exchange rates of ecosystems: past, present and future. Glob. Change Biol. 9, 479–492.

Barbour, M.M., Buckley, T.N., 2007. The stomatal response to evaporative demand persists at night in Ricinus communis plants with high nocturnal conductance. Plant Cell Environ. 30, 711–721.

Battipaglia, G., Saurer, M., Cherubini, P., Calfapietra, C., McCarthy, H.R., Norby, R.J., Francesca Cotrufo, M., 2013. Elevated CO_2 increases tree-level intrinsic water use efficiency: insights from carbon and oxygen isotope analyses in tree rings across three forest FACE sites. New Phytol. 197, 544–554.

Boegelein, R., Hassdenteufel, M., Thomas, F.M., Werner, W., 2012. Comparison of leaf gas exchange and stable isotope signature of water-soluble compounds along canopy gradients of co-occurring Douglas-fir and European beech. Plant Cell Environ. 35, 1245–1257.

Borella, S., Leuenberger, M., Saurer, M., Siegwolf, R., 1998. Reducing uncertainties in δ13C analysis of tree rings: pooling, milling, and cellulose extraction. J. Geophys. Res.: Atmos. 103, 19519–19526.

Bowling, D.R., Sargent, S.D., Tanner, B.D., Ehleringer, J.R., 2003. Tunable diode laser absorption spectroscopy for stable isotope studies of ecosystem–atmosphere CO_2 exchange. Agric. For. Meteorol. 118, 1–19.

Campbell, G.S., Norman, J.M., 2012. An Introduction to Environmental Biophysics. Springer Science & Business Media.

Canadell, J., Mooney, H., Baldocchi, D., Berry, J., Ehleringer, J., Field, C., Gower, S.T., Hollinger, D., Hunt, J., Jackson, R.B., 2000. Commentary: carbon metabolism of the terrestrial biosphere: a multitechnique approach for improved understanding. Ecosystems 3, 115–130.

Catovsky, S., Holbrook, N., Bazzaz, F., 2002. Coupling whole-tree transpiration and canopy photosynthesis in coniferous and broad-leaved tree species. Can. J. For. Res. 32, 295–309.

Cernusak, L.A., Ubierna, N., Winter, K., Holtum, J.A., Marshall, J.D., Farquhar, G.D., 2013. Environmental and physiological determinants of carbon isotope discrimination in terrestrial plants. New Phytol. 200, 950–965.

Ciais, P., Tans, P.P., Trolier, M., White, J.W.C., Francey, R.J., 1995. A large northern hemisphere terrestrial CO_2 sink indicated by the $^{13}C/^{12}C$ ratio of atmospheric CO_2. Science 269, 1098–1102.

Dawson, T.E., Mambelli, S., Plamboeck, A.H., Templer, P.H., Tu, K.P., 2002. Stable isotopes in plant ecology. Annu. Rev. Ecol. Syst. 33, 507–559.

Di Matteo, G., De Angelis, P., Brugnoli, E., Cherubini, P., Scarascia-Mugnozza, G., 2010. Tree-ring Δ13C reveals the impact of past forest management on water-use efficiency in a Mediterranean oak coppice in Tuscany (Italy). Ann. For. Sci. 67, 510.

Evans, J.R., Von Caemmerer, S., 2013. Temperature response of carbon isotope discrimination and mesophyll conductance in tobacco. Plant Cell Environ. 36, 745–756.

Ewers, B., Gower, S., Bond-Lamberty, B., Wang, C., 2005. Effects of stand age and tree species on canopy transpiration and average stomatal conductance of boreal forests. Plant Cell Environ. 28, 660–678.

Ewers, B., Oren, R., Kim, H.S., Bohrer, G., Lai, C.T., 2007. Effects of hydraulic architecture and spatial variation in light on mean stomatal conductance of tree branches and crowns. Plant Cell Environ. 30, 483–496.

Fang, J.Y., Chen, A.P., Peng, C.H., Zhao, S.Q., Ci, L.J., 2001. Changes in forest biomass carbon storage in china between 1949 and 1998. Science 292, 2320–2322.

Farquhar, G.D., Ehleringer, J.R., Hubick, K.T., 1989. Carbon isotope discrimination and photosynthesis. Annu. Rev. Plant Biol. 40, 503–537.

Farquhar, G.D., Sharkey, T.D., 1982. Stomatal conductance and photosynthesis. Annu. Rev. Plant Physiol. 33, 317–345.

Fernández, M.E., Gyenge, J., Schlichter, T., 2009. Water flux and canopy conductance of natural versus planted forests in Patagonia, South America. Trees 23, 415–427.

Forster, M.A., 2014. How significant is nocturnal sap flow? Tree Physiol. 34, 757–765.

Gebremichael, M., Barros, A.P., 2006. Evaluation of MODIS gross primary productivity (GPP) in tropical monsoon regions. Remote Sens. Environ. 100, 150–166.

Granier, A., 1987. Evaluation of transpiration in a Douglas-fir stand by means of sap flow measurements. Tree Physiol. 3, 309–320.

Granier, A., Biron, P., Köstner, B., Gay, L., Najjar, G., 1996. Comparisons of xylem sap flow and water vapour flux at the stand level and derivation of canopy conductance for Scots pine. Theor. Appl. Climatol. 53, 115–122.

Granier, A., Loustau, D., Bréda, N., 2000. A generic model of forest canopy conductance dependent on climate, soil water availability and leaf area index. Ann. For. Sci. 57, 755–765.

Gu, F., Cao, M., Wen, X., Liu, Y., Tao, B., 2006. A comparison between simulated and measured CO_2 and water flux in a subtropical coniferous forest. Sci. China Ser. D: Earth Sci. 49, 241–251.

Holmes, R.L., 1983. Computer-assisted Quality Control in Tree-ring Dating and Measurement. Tree-ring Bulletin.

Hu, J., Moore, D.J., Riveros-Iregui, D.A., Burns, S.P., Monson, R.K., 2010. Modeling whole-tree carbon assimilation rate using observed transpiration rates and needle sugar carbon isotope ratios. New Phytol. 185, 1000–1015.

Jijun, H., Qiangguo, C., Guoqiang, L., Zhongke, W., 2010. Integrated erosion control measures and environmental effects in rocky mountainous areas in northern China. Int. J. Sedim. Res. 25, 294–303.

Johnson, W.C., Sharpe, D.M., 1983. The ratio of total to merchantable forest biomass and its application to the global carbon budget. Can. J. For. Res. 13, 372–383.

Klein, T., Rotenberg, E., Tatarinov, F., Yakir, D., 2016. Association between sap flow-derived and eddy covariance-derived measurements of forest canopy CO_2 uptake. New Phytol. 209, 436–446.

Köstner, B.M.M., Schulze, E.-D., Kelliher, F., Hollinger, D., Byers, J., Hunt, J., McSeveny, T., Meserth, R., Weir, P., 1992. Transpiration and canopy conductance in a pristine broad-leaved forest of Nothofagus: an analysis of xylem sap flow and eddy correlation measurements. Oecologia 91, 350–359.

Leavitt, S.W., 2008. Tree-ring isotopic pooling without regard to mass: no difference from averaging δ13C values of each tree. Chem. Geol. 252, 52–55.

Li, X., He, Y., Wu, X., Ren, Q., 2011. Water stress experiments of Platycladus orientalis and Pinus tablaeformis young trees. For. Res. 24, 91–96.

Liu, Y., Wang, R., Leavitt, S.W., Song, H., Linderholm, H.W., Li, Q., An, Z., 2012. Individual and pooled tree-ring stable-carbon isotope series in Chinese pine from the Nan Wutai region, China: common signal and climate relationships. Chem. Geol. 330, 17–26.

Loader, N., Robertson, I., Barker, A., Switsur, V., Waterhouse, J., 1997. An improved technique for the batch processing of small wholewood samples to α-cellulose. Chem. Geol. 136, 313–317.

Lu, P., Yunusa, I.A., Walker, R.R., Müller, W.J., 2003. Regulation of canopy conductance and transpiration and their modelling in irrigated grapevines. Funct. Plant Biol. 30,

689–698.
Ma, L., 2008. Transpiration of Acacia mangium and It's Coupling to Environmental Factors at Different Temporal and Spatial Scales. Graduate School of the Chinese Academy of Sciences, Beijing, China (Chinese with English Abstract).
Maseyk, K., Hemming, D., Angert, A., Leavitt, S.W., Yakir, D., 2011. Increase in water-use efficiency and underlying processes in pine forests across a precipitation gradient in the dry Mediterranean region over the past 30 years. Oecologia 167, 573–585.
Matheny, A.M., Bohrer, G., Garrity, S.R., Morin, T.H., Howard, C.J., Vogel, C.S., 2015. Observations of stem water storage in trees of opposing hydraulic strategies. Ecosphere 6, 1–13.
McCarroll, D., Loader, N.J., 2004. Stable isotopes in tree rings. Quat. Sci. Rev. 23, 771–801.
Morén, A.-S., Lindroth, A., Grelle, A., 2001. Water-use efficiency as a means of modelling net assimilation in boreal forests. Trees-Struct. Funct. 15, 67–74.
Niinemets, Ü., 2010. A review of light interception in plant stands from leaf to canopy in different plant functional types and in species with varying shade tolerance. Ecol. Res. 25, 693–714.
Niinemets, Ü., Diaz-Espejo, A., Flexas, J., Galmes, J., Warren, C.R., 2009. Role of mesophyll diffusion conductance in constraining potential photosynthetic productivity in the field. J. Exp. Bot. 60, 2249–2270.
Niinemets, Ü., Flexas, J., Peñuelas, J., 2011. Evergreens favored by higher responsiveness to increased CO_2. Trends Ecol. Evol. 26, 136–142.
Nock, C.A., Baker, P.J., Wanek, W., Leis, A., Grabner, M., Bunyavejchewin, S., Hietz, P., 2011. Long-term increases in intrinsic water-use efficiency do not lead to increased stem growth in a tropical monsoon forest in western Thailand. Glob. Change Biol. 17, 1049–1063.
Nowak, D.J., Stevens, J.C., Sisinni, S.M., Luley, C.J., 2002. Effects of urban tree management and species selection on atmospheric carbon dioxide. J. Arboric. 28, 113–122.
Oren, R., Ellsworth, D.S., Johnsen, K.H., Phillips, N., Ewers, B.E., Maier, C., Schäfer, K.V., McCarthy, H., Hendrey, G., McNulty, S.G., 2001. Soil fertility limits carbon sequestration by forest ecosystems in a CO_2-enriched atmosphere. Nature 411, 469.
Osmond, C.B., Björkman, O., Anderson, D.J., 2012. Physiological Processes in Plant Ecology: Toward a Synthesis with Atriplex. Springer Science & Business Media.
Pachauri, R.K., Allen, M.R., Barros, V.R., Broome, J., Cramer, W., Christ, R., Church, J.A., Clarke, L., Dahe, Q., Dasgupta, P., 2014. Climate Change 2014: Synthesis Report. Contribution of Working Groups I, II and III to the Fifth Assessment Report of the Intergovernmental Panel on Climate Change. IPCC.
Peng, S., 2003. Study and Application of Restoration Ecology in Tropical and Subtropical China. Science Press, Beijing, pp. 1–25.
Rayment, M., Jarvis, 1999. Seasonal gas exchange of black spruce using an automatic branch bag system. Can. J. For. Res. 29, 1528–1538.
Resco de Dios, V., Loik, M.E., Smith, R., Aspinwall, M.J., Tissue, D.T., 2016. Genetic variation in circadian regulation of nocturnal stomatal conductance enhances carbon assimilation and growth. Plant Cell Environ. 39, 3–11.
Robertson, I., Leavitt, S.W., Loader, N.J., Buhay, W., 2008. Progress in isotope dendroclimatology. Chem. Geol. 252, EX1–EX4.
Schäfer, K., Oren, R., Tenhunen, J., 2000. The effect of tree height on crown level stomatal conductance. Plant Cell Environ. 23, 365–375.
Silva, L.C., Horwath, W.R., 2013. Explaining global increases in water use efficiency: why have we overestimated responses to rising atmospheric CO_2 in natural forest ecosystems? PLoS One 8, e53089.
Sun, F., Kuang, Y., Wen, D., Xu, Z., Li, J., Zuo, W., Hou, E., 2010. Long-term tree growth rate, water use efficiency, and tree ring nitrogen isotope composition of Pinus massoniana L. in response to global climate change and local nitrogen deposition in Southern China. J. Soils Sedim. 10, 1453–1465.
Szymczak, S., Joachimski, M., Bräuning, A., Hetzer, T., Kuhlemann, J., 2012. Are pooled tree ring δ13C and δ18O series reliable climate archives? – a case study of Pinus nigra spp. laricio (Corsica/France). Chem. Geol. 308, 40–49.
Wang, H., Zhao, P., Zou, L., McCarthy, H., Zeng, X., Ni, G., Rao, X., 2014. CO_2 uptake of a mature Acacia mangium plantation estimated from sap flow measurements and stable carbon isotope discrimination. Biogeosciences 11, 1393.
Wang, X., Ma, L., Jia, Z.K., Xu, C., Zhang, Y., 2005. Primary study on distribution pattern change of Pinus tabulaeformis and Platycladus orientalis plantations in mountainous area of Beijing. J. Southwest For. Coll. 22, 23–26.
Weiwei, L., Xinxiao, Y., Guodong, J., Hanzhi, L., Ziqiang, L., 2018. Responses of intrinsic water-use efficiency and tree growth to climate change in semi-arid areas of North China. Sci. Rep. 8, 308.
Wingate, L., Ogée, J., Burlett, R., Bosc, A., Devaux, M., Grace, J., Loustau, D., Gessler, A., 2010. Photosynthetic carbon isotope discrimination and its relationship to the carbon isotope signals of stem, soil and ecosystem respiration. New Phytol. 188, 576–589.
Woodley, E.J., Loader, N., McCarroll, D., Young, G., Robertson, I., Gagen, M., 2012. Estimating uncertainty in pooled stable isotope time-series from tree-rings. Chem. Geol. 294, 243–248.
Wu, G., Liu, X., Chen, T., Xu, G., Wang, W., Zeng, X., Zhang, X., 2015. Elevation-dependent variations of tree growth and intrinsic water-use efficiency in Schrenk spruce (Picea schrenkiana) in the western Tianshan Mountains, China. Front. Plant Sci. 6, 309.
Zeppel, M., Lewis, J.D., Phillips, N.G., Tissue, D.T., 2014. Consequences of nocturnal water loss: a synthesis of regulating factors and implications for capacitance, embolism and use in models. Tree Physiol. 34, 1047–1055.
Zhang, J., 2012. Study on Biomass Model of P. orientalis in Miaofengshan. Beijing Forestry University, Beijing.
Zhang, X., Li, H., He, J., Wang, Q., Golabi, M.H., 2009a. Influence of conservation tillage practices on soil properties and crop yields for maize and wheat cultivation in Beijing, China. Soil Res. 47, 362–371.
Zhang, X., Wang, M., Liang, X., 2009b. Quantitative classification and carbon density of the forest vegetation in Lüliang Mountains of China. Plant Ecol. 201, 1–9.
Zhao, M., Zhou, G.-S., 2006. Carbon storage of forest vegetation in China and its relationship with climatic factors. Clim. Change 74, 175–189.